Carbon monoxide shifts energetic metabolism from glycolysis to oxidative phosphorylation in endothelial cells

Short title: 'CO inhibits glycolysis and activates OXPHOS in the endothelium'

Patrycja Kaczara[1], Roberto Motterlini[2], Agnieszka Zakrzewska[1], Andrey Y. Abramov[3,*], Stefan Chlopicki[1,*]

*corresponding authors

[1]Jagiellonian Centre for Experimental Therapeutics (JCET), Jagiellonian University, Krakow 30-348, Poland

[2]INSERM Unit 955, Equipe 12, University Paris-Est, Faculty of Medicine, Créteil, 94000, France

[3]Department of Molecular Neuroscience, UCL Institute of Neurology, Queen Square, London WC1N 3BG, UK

*correspondence:

Prof. Stefan Chlopicki, MD,PhD
Bobrzynskiego, 14
30-348 Krakow, Poland
Phone: +48 126645464
e-mail: stefan.chlopicki@jcet.eu

Prof. Andrey Y. Abramov
Queen Square
London WC1N 3BG
Phone: +442034484062
e-mail: a.abramov@ucl.ac.uk

Abstract

Carbon monoxide (CO) modulates mitochondrial respiration but the mechanisms involved are not completely understood. The aim of the present study was to investigate the acute effects of CO on bioenergetics and metabolism in intact EA.hy926 endothelial cells using live cell imaging techniques. CORM-401, a compound that liberates CO, reduced ATP production from glycolysis and induced a mild mitochondrial depolarization, increase mitochondrial calcium and activation of complexes I- and II-dependent mitochondrial respiration leading to ATP production through increased oxidative phosphorylation. Our results show that non-activated endothelial cells rely primarily on glycolysis, but in the presence of CO, mitochondrial Ca^{2+} increases and activates respiration that shift metabolism of endothelial cells from glycolysis- to oxidative phosphorylation–derived ATP production.

Keywords:

Carbon monoxide, CO-RM, endothelium, respiration, oxidative phosphorylation, glycolysis

Abbreviations: CO, carbon monoxide; CO-RMs, CO-releasing molecules; CORM-401, Mn(CO)4{S2CNMe(CH2CO2H)}; iCORM-401, inactive CORM-401; NAD+/NADH, nicotinamide adenine dinucleotide, respectively oxidised/reduced form; FAD/FADH2, flavin adenine dinucleotide, respectively oxidised/reduced form; ETC, electron transport chain; ATP, adenosine triphosphate; ROS; IAA, iodoacetic acid; $\Delta\Psi_m$, mitochondrial membrane potential; FCCP, carbonyl cyanide 4-(trifluoromethoxy)phenylhydrazone; Rh123, Rhodamine 123; TMRM, tetramethylorhodamine; HET, hydroethidium; ECs, endothelial cells; PDH, pyruvate dehydrogenase; PFKFB3, phosphofructokinase/ fructosebisphosphatase; OXPHOS, oxidative phosphorylation; NO, nitric oxide;

22

23 **1. Introduction**

24 There is overwhelming evidence that endogenous carbon monoxide (CO) affords beneficial
25 antioxidant, anti-inflammatory and cytoprotective effects that could be mimicked by carbon
26 monoxide-releasing molecules (CO-RMs) [1–3]. Indeed, CO liberated from CO-RMs has been shown
27 to exert cardio- and vaso-protective effects, as well anti-thrombotic, anti-platelet and anti-
28 inflammatory effects [4–9].

29 The mechanisms of action of CO derived from CO-RMs are not well understood. A series of
30 targets responsive to CO has been identified including guanylate cyclase, mitochondrial cytochromes,
31 potassium channels, NO synthase, NADPH oxidase or transcription factors such as BACH1 or NPAS2
32 [3,10–12]. The peculiar feature of all these CO-responsive targets is that they contain a heme moiety
33 or a transition metal as a prosthetic group. Taking into consideration that CO binds with a high
34 affinity to Fe(II)-heme, it is conceivable that the mitochondrial electron transport chain (ETC), which
35 consists of a number of heme-containing proteins, represents a suitable cellular compartment
36 whereby CO could transduce many of its known physiological effects. Despite some of the functional
37 consequences of CO on mitochondrial bioenergetics have been reported, the specific molecular
38 target(s) and the mode of action of CO within the ETC still remain to be fully investigated [13–19]. At
39 high concentrations, CO is known to inhibit mitochondrial respiration as it strongly competes with
40 oxygen for the binding to cytochrome c oxidase [17–20]. However, in a couple of recent studies
41 conducted mainly on isolated mitochondrial preparations, it was demonstrated that CO, delivered at
42 low micromolar concentrations using CO-RMs or CO gas, uncoupled mitochondrial respiration and
43 increased oxygen consumption rate [14–16]. Lo Iacono et al [14] reported that the uncoupling effect
44 induced by CO was associated with a gradual decrease in mitochondrial membrane potential over
45 time and was partially reversed by inhibition of complex II activity. Long et al. [15] demonstrated that
46 CO activated the phosphate carrier in the inner mitochondrial membrane leading to an increase in
47 phosphate and proton transport inside mitochondria that contributed to the uncoupling effects of
48 CO. Although Reiter et al. [21] and Wegiel et al. [22] previously showed that in intact cells CO also
49 accelerated oxygen consumption rate, these authors did not elucidate the mechanisms of this effect.
50 In our recent study we found that in intact endothelial cells CO liberated from CORM-401, a new
51 manganese-containing CO releaser [23], induced an increase in oxygen consumption rate (OCR) that
52 was accompanied by inhibition of glycolysis (extracellular acidification rate, ECAR) and a mild
53 uncoupling effect as evidenced by an increase in proton leak [24]. Furthermore, CORM-401
54 decreased the mitochondrial reserve capacity and enhanced non-mitochondrial respiration. Blockade

55 of mitochondrial large-conductance calcium-regulated potassium ion channels (mitoBKCa) markedly
56 attenuated the increase in OCR promoted by CORM-401 without affecting ECAR. These results
57 suggested that in intact endothelial cells CO induced a two-component metabolic response:
58 uncoupling of mitochondrial respiration, dependent on activation of mitochondrial BKCa channels,
59 and inhibition of glycolysis independent of mitoBKCa channels.

60 In order to better understand this two-component metabolic response induced by CO in the
61 endothelium, here we investigated the acute effect of CO on bioenergetics in intact endothelial cells
62 using live cell imaging techniques. Taking advantage of this approach we evaluated the immediate
63 effects of CO on the activity of mitochondrial complex I and II and investigated whether this effects
64 of CO is linked to changes in ATP synthesis, ROS production and mitochondrial Ca^{2+} flux.

65

66

67 ## 2. Materials and methods

68 ### *2.1. Reagents*

69 Dulbecco's Modified Eagle Medium (DMEM), fetal bovine serum (FBS), GlutaMAX, HAT
70 supplement, penicillin/streptomycin, sodium pyruvate, and trypsin were obtained from Gibco.
71 Oligomycin, carbonyl cyanide 4-(trifluoromethoxy)phenylhydrazone (FCCP), sodium cyanide,
72 iodoacetic acid (IAA), manganese (II) sulfate (MnSO4) were obtained from Sigma. Fluorescent dyes:
73 Rhodamine 123, Tetramethylorhodamine (TMRM), Hydroethidium (HET) were obtained from
74 Invitrogen. The Effectene Transfection kit was obtained from Qiagen. CORM-401 was synthesized as
75 described previously (Crook 2011). All experiments were performed with using 30 µM CORM-401,
76 selected based on our previous work [24] as concentration at which released carbon monoxide
77 induces a slight acceleration of oxygen consumption rate in EA.hy926 cells.

78

79 ### *2.2. Cell culture*

80 The hybridoma endothelial EA.hy926 cell line, formed by fusion of human umbilical vein
81 endothelial cells (HUVEC) with the A549 human lung carcinoma cell line, was kindly provided by Dr.
82 C-J Edgell (Department of Pathology, University of North Carolina, Chapel Hill, NC, USA) [25]. Cells
83 were propagated using three weekly feedings of DMEM containing 10% FBS, 1 g/l glucose, 110 mg/l
84 sodium pyruvate, 2 mM GlutaMAX™, antibiotics (100 IU penicillin, 100 µg/ml streptomycin) and 2%
85 HAT Supplement. Cultures were maintained at 37 °C in a fully humidified atmosphere of 5% CO_2 in
86 air. Cells were confirmed to be contamination-free. For live cell imaging analysis, cells were plated
87 into 25 mm coverslips in six-well plates to get a density of 80-100%. Before the experiments cells
88 were washed one time with HBSS buffer (156 mM NaCl, 3 mM KCl, 1.25 mM KH_2PO_4, 2 mM $MgSO_4$, 2
89 mM $CaCl_2$, 10 mM glucose, 10 mM HEPES, pH 7.35) and placed into the chamber for staining with a
90 fluorescent dye before recording.

91 ### *2.3. Imaging of $\Delta\Psi_m$, NADH, FAD, ROS generation, intracellular pH and ATP level*

92 For the measurement of $\Delta\Psi_m$, cells were loaded with 1 µg/ml rhodamine123 (Rh123) for 30
93 min at room temperature, and the dye was washed prior to the experiment. An increase in the
94 Rh123 signal reflects mitochondrial depolarization. For the measurement of $\Delta\Psi_m$ using confocal
95 microscopy, cells were loaded with 25 nM tetramethyl rhodamine methylester (TMRM) for 40 min at
96 room temperature and the fluorescent indicator was present in all solutions during the experiment.
97 A decrease in TMRM signal reflects mitochondrial depolarization.

98 Measurements of NADH autofluorescence were performed by using excitation light of a
99 wavelength 360 nm and emitted fluorescence light was reflected through a 455 nm long-pass filter
100 [26]. FAD autofluorescence was monitored using a confocal microscopy. Excitation at 454 nm was
101 performed using an Argon laser line and fluorescence was measured from 505 to 550 nm.

102 The assessment of ROS generation was performed using hydroethidine (HET) (2 µM), which
103 was present in all solutions throughout the experiments. No pre-loading was used to limit the
104 intracellular accumulation of oxidized products.

105 Intracellular ATP levels were assessed by confocal microscopy. Briefly, Ea.hy926 cells were
106 transfected with a genetically encoded ATP indicator AT1.03 cDNA [27] using an Effectene
107 transfection reagent (Qiagen). AT.103 measures only free ATP and not Mg^{2+}-bound ATP. One day
108 after transfection, cells were subjected to imaging and ratio-metric analysis of the yellow- (λ_{ex}=405
109 nm, λ_{em}=515-580 nm) and cyan-fluorescent (λ_{ex}=405 nm, λ_{em}=460-510 nm) proteins was performed.

110 The energy capacity of cells was assessed by measuring the time needed for total ATP
111 consumption after treatment of cells with a combination of inhibitors of glycolysis (20 µM iodoacetic
112 acid, IAA) and oxidative phosphorylation (1 mM NaCN), which blocked ATP production and lead to
113 ATP depletion. Upon hydrolysis of ATP magnesium (Mg^{2+}) is released from MgATP, and therefore live
114 cell imaging of cellular free magnesium ($[Mg^{2+}]_c$) using the Mg^{2+}-sensitive fluorescent probe MagFura-
115 2 can be used as an indicator of ATP consumption [28,29]. For the measurement of free $[Mg^{2+}]_c$ level
116 cells were loaded with 5 µM MagFura-2 and 0.005 % Pluronic for 30 min at room temperature. A
117 ratio of emission intensity at 515 nm was determined when the dye was excited at 340 nm versus
118 380 nm

119 Fluorescence measurements were performed using either a epifluorescence inverted
120 microscope equipped with a cooled CCD camera or with a Zeiss (Oberkochen, Germany) 710 VIS
121 CLSM. To achieve reproducible data the cells from periphery of the slide were excluded from
122 analysis.

123 Confocal images were obtained with using 40x or 63x oil immersion objective. Excitation was
124 measured from 505 to 550 nm. Illumination intensity was kept to a minimum (at 0.1 – 0.2% of laser
125 output) to avoid phototoxicity and the pinhole set to give an optical slice of ~2µm.

126 *2.4. Analysis of 2-hydroxyethidium (2-OH-E^+) by HPLC with fluorescence and UV-visible absorption*
127 *detection*

128 Detection of 2-hydroxyethidium (2-OH-E^+), a specific product of superoxide ($O_2^{\bullet-}$) reaction
129 with hydroethidine (HET) in cellular system was performed according to a modified protocol
130 described by [30]. Briefly, confluent EA.hy926 cells (85 mm dishes) were incubated for 30 min with
131 10 μM HET. Extraction of hydroethidine derivatives were analysed by HPLC with fluorescence
132 detection performed using UFLC Nexera system (Shimadzu, Kyoto, Japan). Chromatographic
133 separation was carried out on a Kinetex C18 analytical column (4.6x100mm, 2.6μm, Phenomenex,
134 Torrance, CA, USA) with the oven temperature set at 40 °C. The autosampler temperature was
135 maintained at 4 °C. The mobile phase consisted of acetonitrile (A) and water (B) both with an
136 addition of 0.1 % trifluoroacetic acid with the following linear eluting steps: 0.0 min (A:B, 25/75, v/v)
137 – 0.5 min (A:B, 25/75, v/v) – 8 min (A:B, 35/65, v/v) – 9 min (A:B, 95/5, v/v) – 11 min (A:B, 95/5, v/v) –
138 12.0 min (A:B, 25/75, v/v) – 14.0 min (A:B, 25/75, v/v). The flow rate was set at 1 ml min^{-1}. A sample
139 volume of 50 μl was injected onto column. The linearity range of the method was 0.005-0.5 μM.

140 *2.5. Statistics*

141 Statistical analysis was performed using a OriginPro 9.1 software (OriginLab Corporation).
142 Results were expressed as means ± s.e.m. For statistical analysis One-way ANOVA with Benferroni's
143 Multiple Comparison Test was performed, *P* values provided in the legends.

144

145

146 **3. Results**

147 *3.1. CORM-401 shifts ATP production from glycolysis to oxidative phosphorylation in endothelial*
148 *cells.*

149 To verify the effect of CO on energy production in endothelial cells, we first measured
150 cytosolic ATP concentration using a genetically encoded fluorescent ATP indicator (AT1.03). We
151 found that after addition of the ATP-synthase inhibitor oligomycin (2 µg/ml), the ATP content in
152 untreated EA.hy926 cells or in cells treated with an inactive CORM-401 that does not release CO
153 (iCORM-401) remained almost unchanged. However, ATP rapidly decreased after inhibition of
154 glycolysis with 20 µM iodoacetic acid (IAA, glyceraldehyde 3-phosphate dehydrogenase inhibitor; Fig.
155 1A,B) indicating that endothelial cells rely mainly on glycolysis for ATP production [31,32]. In
156 contrast, in endothelial cells treated with CO liberated from CORM-401, oligomycin induced a rapid
157 (3 min) and significant decrease in intracellular ATP concentration that was further diminished after
158 application of IAA (Fig. 1C). These results suggest that the contribution to ATP production by
159 oxidative phosphorylation in endothelial cells is considerably increased in the presence of CO. To
160 verify whether CO affected the energy capacity of the cell, we assessed the time period required for
161 energetic collapse (i.e. total intracellular ATP pool depletion) and breakdown of calcium homeostasis
162 [29] following simultaneous inhibition of glycolysis (IAA) and oxidative phosphorylation (NaCN,
163 complex IV inhibitor). Live cell imaging of the fluorescent probe MagFura-2 was employed to assess
164 the energy capacity of endothelial cells treated with CORM-401 or iCORM-401. Magnesium (Mg^{2+}) is
165 released from MgATP upon the hydrolysis of ATP, and therefore measurement of cellular free
166 magnesium ($[Mg^{2+}]_c$) using the Mg^{2+}-sensitive fluorescent probe MagFura-2 is an indicator of ATP
167 consumption [28,29]. Treatment of cells with inhibitors of glycolysis and oxidative phosphorylation
168 blocked ATP production in cells, which eventually lead to ATP depletion, subsequent Mg^{2+} release
169 and MagFura-2 fluorescence increase (Fig. 2A-C). As shown in Fig. 2D CORM-401 did not affect the
170 energy capacity of endothelial cells.

171 3.2. *CORM-401 induces mild depolarization of mitochondria.*

172 The regulatory effect of CORM-401 on endothelial metabolism was associated with a small
173 (~20%) mitochondrial depolarization (Fig. 3A). Mitochondrial membrane potential ($\Delta\Psi_m$) gradually
174 decreased after addition of CORM-401 (note: the increase of Rh123 fluorescence shown in Fig. 3A
175 corresponds to a decrease in $\Delta\Psi_m$). Basal levels of $\Delta\Psi_m$, which was measured with TMRM 10 min
176 after incubation of endothelial cells with CORM-401, was reduced by 20% in comparison to untreated
177 cells or cells treated with iCORM-401 (Fig. 3C-E). Application of FCCP (1 µM) at the end of

178 measurements caused a rapid and complete depolarization of mitochondria. As shown in Fig. 3B,
179 iCORM-401 did not affect $\Delta\Psi_m$, indicating that the depolarization of $\Delta\Psi_m$ observed after
180 administration of CORM-401 was due to CO liberated by CORM-401. As the production of reactive
181 oxygen species (ROS) generation is dependent on $\Delta\Psi_m$, we then studied the acute effects of CORM-
182 401 on ROS generation using the hydroethidine (HET) fluorescence assay. CORM-401 did not change
183 the rate of ROS production in endothelial cells throughout 30 min of incubation, which was also
184 confirmed using live cells imaging technique (Fig. 3F) as well as HPLC-based measurements of 2-
185 hydroxyethidium (2-OH-E^+, see Fig. 3G), a specific product of the reaction between superoxide ($O_2^{\bullet-}$)
186 and HET [30]. In contrast, 10 µM menadione, which is known to generate superoxide (positive
187 control)[33], induced a marked increase in 2-OH-E^+ in endothelial cells (Fig. 3G).

188 Impaired mitochondrial respiration or high glycolytic activity can induce a switch of the F0-
189 F1-ATP synthase to work in reverse mode (as ATPase) in order to maintain $\Delta\Psi_m$ [29], we next
190 examined whether ATP synthase activity was indeed affected by CORM-401. The F0-F1-ATP synthase
191 inhibitor oligomycin was employed to test if CORM-401 affected the mechanism of $\Delta\Psi_m$
192 maintenance. Inhibition of ATP synthase in control endothelial cells induced a significant reduction in
193 $\Delta\Psi_m$ (Fig. 4A) suggesting that F0-F1-ATPase was working in reverse mode (consuming ATP). These
194 results confirm our observation (Fig. 1) that endothelial cells are highly glycolytic and maintain $\Delta\Psi_m$
195 using ATP produced in glycolysis. Importantly, pre-incubation of cells with CORM-401 for 20 min not
196 only reduced $\Delta\Psi_m$ but also decreased the effect of oligomycin on TMRM signal (Fig. 4B). These data
197 suggest that in endothelial cells the production of ATP predominantly from glycolytic sources is
198 shifted to ATP synthesis derived mainly from mitochondrial oxidative phosphorylation in the
199 presence of CO (Fig. 4B) and this effect is associated with a change in F0-F1-ATPase activity from
200 reverse mode (ATPase) to ATP-production mode.

201 3.3. *CORM-401 activates complexes I and II of the electron transport chain (ETC).*

202 The effect of CORM-401 on the respiratory chain activity in endothelial cells was studied by
203 measurement of NADH and FAD autofluorescence. CORM-401 accelerated NADH consumption (Fig.
204 5), induced a fall in NADH redox index, as the total mitochondrial pool of NADH did not change in
205 comparison to the control conditions (iCORM-401; Fig. 5B, C). CORM-401 induced a decrease in
206 NADH autofluorescence (induced by activation of complex I) and this was accompanied by an
207 increase in FAD autofluorescence (induced by activation of the complex II, fig. 5D). These results
208 indicate that not only complex I, but also complex II was activated by CO derived from CORM-401.
209 However, changes in the activities of ETC complexes induced by CORM-401 were relatively rapid, and
210 on the basis of this we hypothesized that this could be due to changes in mitochondrial calcium

211 handling in response to CO (Fig. 6). CORM-401 increased the calcium contents in the matrix of
212 mitochondria as measured by x-rhod-1 fluorescence [34]. This increase in calcium levels may then be
213 responsible for the increase in mitochondrial respiration and activation of the production of ATP by
214 oxidative phosphorylation.

215

216 **4. Discussion**

217 In the present study we investigated the acute effects of CO liberated from CORM-401 on
218 endothelial bioenergetics. We demonstrated that quiescent ECs rely mainly on glycolysis and
219 maintain mitochondrial membrane potential by glycolysis-derived ATP and F0-F1-ATP synthase
220 working in a reverse mode (ATPase). In contrast, addition of CO at low micromolar concentrations
221 resulted in a mild uncoupling effect that was accompanied by a shift in endothelial metabolism from
222 glycolysis to mitochondrial respiration leading to increased ATP production derived mainly from
223 oxidative phosphorylation. These results indicate that CO fine-tunes the bioenergetic profile of
224 endothelial cells, which may have important implications in both physiological and
225 pathophysiological processes.

226 The finding that CO induces activation of respiration under physiological conditions is
227 intriguing and rather counterintuitive. In fact, high concentrations of CO potently inhibit complex IV
228 activity within the ETC due to its high competition with oxygen for the binding site [17–20]. However,
229 a number of reports have now emerged showing that CO delivered in controlled amounts does not
230 inhibit respiration but rather promotes a transient increase in oxygen consumption in isolated
231 mitochondria from various organs or different cell types including cardiomyocytes, astrocytes and
232 hepatocytes [13–15,35,36]. The mechanisms responsible for this effect are at present not completely
233 understood. We have demonstrated in one of our recent studies that CO in intact ECs exhibits two
234 independent but simultaneous effects: acceleration of mitochondrial respiration mediated by
235 activation of mitoBKCa channels and inhibition of glycolysis independent of mitoBKCa channels [24].
236 In the present report we confirmed that CO from CORM-401 increased mitochondrial respiration and
237 demonstrated for the first time that this effect involved an increase in the activity of complexes I and
238 II in ETC. Previously, in studies conducted on isolated rat heart mitochondria, Lo Iacono and
239 colleagues found that CO released by CORM-3 at concentrations between 1 and 20 µM increased
240 state 2 mitochondrial respiration through an uncoupling effect, although no direct effect was found
241 on the activity of the ETC complexes [14]. However, treatment of isolated mitochondria with
242 malonate, an inhibitor of complex II, reversed the increase in state 2 respiration induced by CORM-3
243 suggesting that complex II activity, most likely indirectly, can be modulated by CO. In our study
244 performed in intact endothelial cells, thus preserving the natural intracellular milieu, CO liberated by
245 CORM-401 accelerated the consumption of NADH that is provided by the tricarboxylic acid (TCA)
246 cycle. It is known that changes in the activity of the ETC complexes may affect the TCA cycle turnover
247 through bidirectional feedback mechanisms on pyruvate dehydrogenase, which is regulated by
248 NAD+/NADH ratio [37]. Accordingly, the results of the present study suggest that increased
249 consumption of mitochondrial NADH induced by CO is linked to the activation of TCA. In this context,

250 it was interesting to observe that CO induced an increase in mitochondrial calcium content. Calcium
251 activates diverse cellular ATP-consuming processes, as well as pyruvate dehydrogenase and other
252 mitochondrial dehydrogenases orchestrating the supply of NADH to ETC. These enzymes provide a
253 constant reducing power in the form of NADH that are utilized by the mitochondrial ETC to sustain
254 energy demand [38]. Thus, although other mechanisms could also be involved [39,40], the activation
255 of both complexes I and II by CO reported was linked here with a transient increase in mitochondrial
256 calcium and concomitantly to an accelerated TCA turnover. Altogether, our results suggest that CO
257 released by CORM-401 induces an activation of complexes I and II as a result of increased
258 mitochondrial calcium content and subsequent acceleration of TCA cycle turnover.

259 An interesting finding of this work was that the acute effects of CO on mitochondrial
260 respiration were associated with a rapid metabolic shift from glycolysis to oxidative phosphorylation,
261 which in turn did not affect the energy capacity of the cell. The inhibitory effect of CO on glycolysis is
262 in accordance with the work published by Yamamoto et al. [41]. Authors reported that CO affected
263 glycolysis by inhibition of cystathionie β-synthase and subsequent reduction in
264 phosphofructokinase/fructosebisphosphatase type3 (PFKFB3) methylation leading to a shunt of
265 glucose from glycolysis to the pentose phosphate pathway. Interestingly, PFKFB3 has been suggested
266 as a key regulatory enzyme in the control of endothelial glycolysis [32,42,43]. The reprogramming of
267 cells in energy production reported here occurred quite rapidly – as early as 3 min after addition of
268 CORM-401 and was sustained for over 30 min (Fig. 1) - and constitutes qualitatively different
269 response as observed previously [24] 50 min after addition of CORM-401. Accordingly, the different
270 effects of CO in these two situations depended not only on CO concentration, but also on the time of
271 exposure, suggesting that CO may have transient and sustained effects on mitochondrial function.
272 Most importantly, our data presented here indicate that despite a partial inhibition of glycolysis by
273 CO, endothelial cells rapidly adjust their metabolism to energetic demands. Thus, we demonstrated
274 for the first time that CO at low concentrations is able to fine-tune endothelial cell metabolism. This
275 effect may have an important physiological significance in the protective properties attributed to CO,
276 which could function as intracellular regulator of metabolism in energy-consuming defensive
277 processes against stress conditions.

278 There are number of reports showing an increased production of ROS following exposure of
279 cells and tissues to CO [12–14,18,22]. Here, we found that CO did not accelerate the production of
280 ROS (Fig. 3F,G). These results, together with a mild decrease of mitochondrial membrane potential
281 ($\Delta\Psi_m$) (Fig. 3A) and an activation of complexes I and II (Fig. 5) highlight that CO at low concentrations
282 has an effect on endothelial bioenergetics that is not linked to alterations in ROS production.

283 Mitochondrial membrane potential ($\Delta\Psi_m$), which is usually maintained by cellular respiration
284 [44], is a key component in the preservation of a mitochondrial function. Here, we demonstrated
285 that after treatment with CORM-401 oligomycin diminished $\Delta\Psi_m$ (Fig. 4A) indicating that before
286 addition of the inhibitor, $\Delta\Psi_m$ was partially maintained by hydrolysis of ATP delivered by cytoplasmic
287 glycolysis and processed by F0-F1-ATP synthase working in reversed mode. At first, these results
288 would indicate some serious dysfunction within the cells possibly due to an increased proton leak
289 through the inner mitochondrial membrane [45]. However, ECs prefer glycolysis for ATP production
290 (for review see [32]). Even though ECs possess functional mitochondria, glycolysis-derived ATP can be
291 utilized for the maintenance of $\Delta\Psi_m$ in functional non-activated ECs. It is tempting to speculate that
292 this is an adaptation of ECs to their role in the vasculature. In fact, $\Delta\Psi_m$ controls not only
293 mitochondrial bioenergetic processes but also a transition between life and death [45,46]. In fact,
294 preservation of $\Delta\Psi_m$ in the endothelium has to be supported by the ATP generating system that is
295 independent of mitochondrial respiration, to avoid a collapse of $\Delta\Psi_m$ induced by endothelium-
296 derived NO. Similar mechanism of $\Delta\Psi_m$ control has also been observed in other cell types, which
297 were able to maintain $\Delta\Psi_m$ by glycolytically-derived ATP after treatment with NO [47,48].

298 In conclusion, to our knowledge, we report here for the first time that CO delivered by
299 CORM-401 induces an acute shift from glycolysis to OXOPHOS in endothelial cells while preserving
300 their ATP producing capacity. CO increases the activity of complexes I and II in the mitochondrial ETC
301 and slightly uncouples mitochondria most likely *via* a calcium-dependent mechanism. A progressive
302 decrease in $\Delta\Psi_m$, which we observed in ECs in response to CO, might be the result of multiple effects
303 occurring in a successive fashion including uncoupling of mitochondrial respiration, proton leak and
304 decreased availability of glycolytically generated ATP. CO-dependent regulation of bioenergetics in
305 the endothelium may constitute an important adjusting mechanism that regulates energetic
306 metabolism to maintain endothelial homeostasis.

307

Acknowledgments

Project financed by Polish National Science Centre, decisions no DEC-2012/05/D/NZ7/02518 and DEC-2013/08/M/MN7/01034. We thank Prof. Brian Mann (University of Sheffield) for the synthesis of CORM-401.

Competing interests

No competing interests declared.

Author contributions

Study design (PK, AYA, SCH), providing experimental tools (AYA,RM, PK, SCH), study execution (PK, AYA, AZ), interpretation of findings (all co-authors), drafting the manuscript (PK, SCH, AYA), revising the manuscript (PK, RM, AYA,SCH)

320

321 **References**

322 [1] R. Motterlini, J.E. Clark, R. Foresti, P. Sarathchandra, B.E. Mann, C.J. Green, Carbon monoxide-
323 releasing molecules: characterization of biochemical and vascular activities., Circ. Res. 90
324 (2002) E17–24. http://www.ncbi.nlm.nih.gov/pubmed/11834719 (accessed February 2, 2016).

325 [2] R. Motterlini, B.E. Mann, R. Foresti, Therapeutic applications of carbon monoxide-releasing
326 molecules, Expert Opin. Investig. Drugs. 14 (2005) 1305–1318.
327 doi:10.1517/13543784.14.11.1305.

328 [3] R. Motterlini, L.E. Otterbein, The therapeutic potential of carbon monoxide., Nat. Rev. Drug
329 Discov. 9 (2010) 728–43. doi:10.1038/nrd3228.

330 [4] I.A. Sammut, R. Foresti, J.E. Clark, D.J. Exon, M.J. Vesely, P. Sarathchandra, et al., Carbon
331 monoxide is a major contributor to the regulation of vascular tone in aortas expressing high
332 levels of haeme oxygenase-1., Br. J. Pharmacol. 125 (1998) 1437–44.
333 doi:10.1038/sj.bjp.0702212.

334 [5] J.E. Clark, P. Naughton, S. Shurey, C.J. Green, T.R. Johnson, B.E. Mann, et al., Cardioprotective
335 actions by a water-soluble carbon monoxide-releasing molecule., Circ. Res. 93 (2003) e2–8.
336 doi:10.1161/01.RES.0000084381.86567.08.

337 [6] R. Foresti, J. Hammad, J.E. Clark, T.R. Johnson, B.E. Mann, A. Friebe, et al., Vasoactive
338 properties of CORM-3, a novel water-soluble carbon monoxide-releasing molecule., Br. J.
339 Pharmacol. 142 (2004) 453–60. doi:10.1038/sj.bjp.0705825.

340 [7] A. Zimmermann, C.W. Leffler, D. Tcheranova, A.L. Fedinec, H. Parfenova, Cerebroprotective
341 effects of the CO-releasing molecule CORM-A1 against seizure-induced neonatal vascular
342 injury., Am. J. Physiol. Heart Circ. Physiol. 293 (2007) H2501–7.
343 doi:10.1152/ajpheart.00354.2007.

344 [8] S. Chlopicki, M. Łomnicka, A. Fedorowicz, E. Grochal, K. Kramkowski, A. Mogielnicki, et al.,
345 Inhibition of platelet aggregation by carbon monoxide-releasing molecules (CO-RMs):
346 comparison with NO donors, Naunyn. Schmiedebergs. Arch. Pharmacol. 385 (2012) 641–50.
347 doi:10.1007/s00210-012-0732-4.

348 [9] K. Kramkowski, A. Leszczynska, A. Mogielnicki, S. Chlopicki, E. Grochal, B. Mann, et al.,
349 Antithrombotic properties of water-soluble carbon monoxide-releasing molecules,
350 Arterioscler. Thromb. Vasc. Biol. 32 (2012) 2149–2157. doi:10.1161/ATVBAHA.112.253989.

351 [10] J. Boczkowski, J.J. Poderoso, R. Motterlini, CO-metal interaction: Vital signaling from a lethal
352 gas., Trends Biochem. Sci. 31 (2006) 614–21. doi:10.1016/j.tibs.2006.09.001.

353 [11] E.M. Dioum, J. Rutter, J.R. Tuckerman, G. Gonzalez, M.-A. Gilles-Gonzalez, S.L. McKnight,
354 NPAS2: a gas-responsive transcription factor., Science. 298 (2002) 2385–7.
355 doi:10.1126/science.1078456.

356 [12] Y.K. Choi, E.D. Por, Y.-G. Kwon, Y.-M. Kim, Regulation of ROS production and vascular function
357 by carbon monoxide., Oxid. Med. Cell. Longev. 2012 (2012) 794237.
358 doi:10.1155/2012/794237.

359 [13] S. Lancel, S.M. Hassoun, R. Favory, B. Decoster, R. Motterlini, R. Neviere, Carbon monoxide
360 rescues mice from lethal sepsis by supporting mitochondrial energetic metabolism and
361 activating mitochondrial biogenesis, J. Pharmacol. Exp. Ther. 329 (2009) 641–648.
362 doi:10.1124/jpet.108.148049.could.

363 [14] L. Lo Iacono, J. Boczkowski, R. Zini, I. Salouage, A. Berdeaux, R. Motterlini, et al., A carbon
364 monoxide-releasing molecule (CORM-3) uncouples mitochondrial respiration and modulates
365 the production of reactive oxygen species, Free Radic. Biol. Med. 50 (2011) 1556–64.
366 doi:10.1016/j.freeradbiomed.2011.02.033.

367 [15] R. Long, I. Salouage, A. Berdeaux, R. Motterlini, D. Morin, CORM-3, a water soluble CO-
368 releasing molecule, uncouples mitochondrial respiration via interaction with the phosphate
369 carrier, Biochim. Biophys. Acta. 1837 (2014) 201–9. doi:10.1016/j.bbabio.2013.10.002.

370 [16] C.S.F. Queiroga, A.S. Almeida, P.M. Alves, C. Brenner, H.L.A. Vieira, Carbon monoxide prevents
371 hepatic mitochondrial membrane permeabilization, BMC Cell Biol. 12 (2011) 10.
372 doi:10.1186/1471-2121-12-10.

373 [17] C.E. Cooper, G.C. Brown, The inhibition of mitochondrial cytochrome oxidase by the
374 gasescarbon monoxide, nitric oxide, hydrogen cyanide and hydrogensulfide: chemical
375 mechanism and physiological significance, J. Bioenerg. Biomembr. 40 (2008) 533–539.

376 [18] B.S. Zuckerbraun, B.Y. Chin, M. Bilban, J.D.C. D'Avila, J. Rao, T.R. Billiar, et al., Carbon
377 monoxide signals via inhibition of cytochrome c oxidase and generation of mitochondrial
378 reactive oxygen species, FASEB J. 21 (2007) 1099–106. doi:10.1096/fj.06-6644com.

379 [19] K. Iheagwara, S. Thom, C. Deutschman, R. Levy, Myocardial cytochrome oxidase activity is
380 decreased following carbon monoxide exposure, Biochim. Biophys. Acta. 1772 (2007) 1112–
381 1116.

382 [20] G. D'Amico, F. Lam, T. Hagen, S. Moncada, Inhibition of cellular respiration by endogenously
383 produced carbon monoxide., J. Cell Sci. 119 (2006) 2291–8. doi:10.1242/jcs.02914.

384 [21] C.E.N. Reiter, A.I. Alayash, Effects of carbon monoxide (CO) delivery by a CO donor or
385 hemoglobin on vascular hypoxia inducible factor 1α and mitochondrial respiration., FEBS
386 Open Bio. 2 (2012) 113–8. doi:10.1016/j.fob.2012.05.003.

387 [22] B. Wegiel, D. Gallo, E. Csizmadia, C. Harris, J. Belcher, G.M. Vercellotti, et al., Carbon
388 monoxide expedites metabolic exhaustion to inhibit tumor growth., Cancer Res. 73 (2013)
389 7009–21. doi:10.1158/0008-5472.CAN-13-1075.

390 [23] S.H. Crook, B.E. Mann, A.J.H.M. Meijer, H. Adams, P. Sawle, D. Scapens, et al.,
391 [Mn(CO)4{S2CNMe(CH2CO2H)}], a new water-soluble CO-releasing molecule., Dalt. Trans. 40
392 (2011) 4230–5. doi:10.1039/c1dt10125k.

393 [24] P. Kaczara, R. Motterlini, G.M. Rosen, B. Augustynek, P. Bednarczyk, A. Szewczyk, et al.,
394 Carbon monoxide released by CORM-401 uncouples mitochondrial respiration and inhibits
395 glycolysis in endothelial cells: A role for mitoBKCa channels., Biochim. Biophys. Acta. 1847
396 (2015) 1297–1309. doi:10.1016/j.bbabio.2015.07.004.

397 [25] C. Edgell, C. McDonald, J. Graham, Permanent cell line expressing human factor VIII-related
398 antigen established by hybridization, Proc. Natl. Acad. Sci. U. S. A. 80 (1983) 3734–7.

399 [26] F. Bartolome, A.Y. Abramov, Measurement of mitochondrial NADH and FAD autofluorescence
400 in live cells, Methods Mol. Biol. 1264 (2015) 263–270.

401 [27] H. Imamura, K.P.H. Nhat, H. Togawa, K. Saito, R. Iino, Y. Kato-Yamada, et al., Visualization of
402 ATP levels inside single living cells with fluorescence resonance energy transfer-based
403 genetically encoded indicators, Proc. Natl. Acad. Sci. U. S. A. 106 (2009) 15651–15656.

404 [28] A. Leyssens, A. V Nowicky, L. Patterson, M. Crompton, M.R. Duchen, The relationship between
405 mitochondrial state, ATP hydrolysis, [Mg2+]i and [Ca2+]i studied in isolated rat

406 cardiomyocytes., J. Physiol. 496 (Pt 1 (1996) 111–28.
407 http://www.pubmedcentral.nih.gov/articlerender.fcgi?artid=1160828&tool=pmcentrez&rend
408 ertype=abstract (accessed February 2, 2016).

409 [29] Z. Yao, S. Gandhi, V.S. Burchell, H. Plun-Favreau, N.W. Wood, A.Y. Abramov, Cell metabolism
410 affects selective vulnerability in PINK1-associated Parkinson's disease., J. Cell Sci. 124 (2011)
411 4194–202. doi:10.1242/jcs.088260.

412 [30] J. Zielonka, J. Vasquez-Vivar, B. Kalyanaraman, Detection of 2-hydroxyethidium in cellular
413 systems: a unique marker product of superoxide and hydroethidine, Nat. Protoc. 3 (2008) 8–
414 21. doi:10.1038/nprot.2007.473.

415 [31] A. Dobrina, F. Rossi, Metabolic properties of freshly isolated bovine endothelial cells.,
416 Biochim. Biophys. Acta. 762 (1983) 295–301.

417 [32] J. Goveia, P. Stapor, P. Carmeliet, Principles of targeting endothelial cell metabolism to treat
418 angiogenesis and endothelial cell dysfunction in disease, EMBO Mol. Med. 6 (2014) 1105–
419 1120. doi:10.15252/emmm.201404156.

420 [33] G.M. Rosen, B. a Freeman, Detection of superoxide generated by endothelial cells., Proc. Natl.
421 Acad. Sci. U. S. A. 81 (1984) 7269–7273. doi:10.1073/pnas.81.23.7269.

422 [34] S. Gandhi, A. Vaarmann, Z. Yao, M.R. Duchen, N.W. Wood, A.Y. Abramov, Dopamine Induced
423 Neurodegeneration in a PINK1 Model of Parkinson's Disease, PLoS One. 7 (2012) e37564.

424 [35] A. Sandouka, E. Baloqun, R. Foresti, B. Mann, T. Johnson, Y. Tayem, et al., Carbon monoxide-
425 releasing molecules (CO-RMs) modulate respiration in isolated mitochondria, Cell. Mol. Biol.
426 51 (2005) 425–432.

427 [36] S.S. Almeida, C.S.F. Queiroga, M.F.Q. Sousa, P.M. Alves, H.L.. Vieira, Carbon monoxide
428 modulates apoptosis by reinforcing oxidative metabolism in astrocytes: role of BCL-2., J. Biol.
429 Chem. 287 (2012) 10761–10770. doi:10.1074/jbc.M111.306738.

430 [37] S.-M. Fendt, E.L. Bell, M.A. Keibler, B.A. Olenchock, J.R. Mayers, T.M. Wasylenko, et al.,
431 Reductive glutamine metabolism is a function of the α-ketoglutarate to citrate ratio in cells.,
432 Nat. Commun. 4 (2013) 2236. doi:10.1038/ncomms3236.

433 [38] R.M. Denton, Regulation of mitochondrial dehydrogenases by calcium ions, Biochim. Biophys.
434 Acta - Bioenerg. 1787 (2009) 1309–1316.

435 [39] K.A. Olson, J.C. Schell, J. Rutter, Pyruvate and Metabolic Flexibility: Illuminating a Path Toward
436 Selective Cancer Therapies, Trends Biochem. Sci. 41 (2016) 219–230.

437 [40] N.M. Vacanti, A.S. Divakaruni, C.R. Green, S.J. Parker, R.R. Henry, T.P. Ciaraldi, et al.,
438 Regulation of Substrate Utilization by the Mitochondrial Pyruvate Carrier, Mol. Cell. 56 (2014)
439 425–435.

440 [41] T. Yamamoto, N. Takano, K. Ishiwata, M. Ohmura, Y. Nagahata, T. Matsuura, et al., Reduced
441 methylation of PFKFB3 in cancer cells shunts glucose towards the pentose phosphate
442 pathway., Nat. Commun. 5 (2014) 3480. doi:10.1038/ncomms4480.

443 [42] K. De Bock, M. Georgiadou, S. Schoors, A. Kuchnio, B.W. Wong, A.R. Cantelmo, et al., Role of
444 PFKFB3-driven glycolysis in vessel sprouting, Cell. 154 (2013) 651–63.
445 doi:10.1016/j.cell.2013.06.037.

446 [43] Y. Xu, X. An, X. Guo, T.G. Habtetsion, Y. Wang, X. Xu, et al., Endothelial PFKFB3 plays a critical
447 role in angiogenesis., Arterioscler. Thromb. Vasc. Biol. 34 (2014) 1231–9.
448 doi:10.1161/ATVBAHA.113.303041.

449 [44] M.R. Duchen, Mitochondria in health and disease: perspectives on a new mitochondrial
450 biology., Mol. Aspects Med. 25 (2004) 365–451. doi:10.1016/j.mam.2004.03.001.

451 [45] D.G. Nicholls, S. Ferguson, Bioenergetics, Fourth Edi, Academic Press, 2013.

452 [46] E. Gottlieb, S.M. Armour, M.H. Harris, C.B. Thompson, Mitochondrial membrane potential
453 regulates matrix configuration and cytochrome c release during apoptosis., Cell Death Differ.
454 10 (2003) 709–17. doi:10.1038/sj.cdd.4401231.

455 [47] A. Almeida, J. Almeida, J.P. Bolaños, S. Moncada, Different responses of astrocytes and
456 neurons to nitric oxide: the role of glycolytically generated ATP in astrocyte protection., Proc.
457 Natl. Acad. Sci. U. S. A. 98 (2001) 15294–9. doi:10.1073/pnas.261560998.

458 [48] B. Beltrán, A. Mathur, M.R. Duchen, J.D. Erusalimsky, S. Moncada, The effect of nitric oxide on
459 cell respiration: A key to understanding its role in cell survival or death., Proc. Natl. Acad. Sci.
460 U. S. A. 97 (2000) 14602–7. doi:10.1073/pnas.97.26.14602.

461

462

463

464 **Figure Legends**

465 **Figure 1**

466 **CORM-401 shifts glycolysis to oxidative phosphorylation in ATP production**. (A-C) Cytosolic ATP in
467 EA.hy926 cells transfected with AT1.03 measured as a fluorescence ratio 527/475 nm in cells
468 untreated (A; n = 8), treated with iCORM-401 (inactive ligand for CORM-401 + $MnSO_4$; 30 µM; B; n =
469 9) or CORM-401 (30 µM) – a compound releasing carbon monoxide (C; n = 14). 2 µg/ml oligomycin
470 was used to inhibit oxidative phosphorylation, 20 µM iodoacetic acid (IAA) to inhibit glycolysis. Data
471 are presented as means in a representative experiment.

472 **Figure 2**

473 **CORM-401 does not affect energy capacity of cells**. (A-C) EA.hy926 cells were untreated (A; n = 149),
474 treated with 30 µM iCORM-401 (B; n = 145 cells) or 30 µM CORM-401 (C; n = 157 cells). ATP
475 depletion was measured with using Mg-sensitive fluorescence probe Mag-Fura-2 after treatment of
476 cells with inhibitors of glycolysis (20 µM iodoacetic acid, IAA) and oxidative phosphorylation (1 mM
477 NaCN), which blocked ATP production in cells. Figures show traces from twelve representative cells in
478 each. (D) Energy capacity reflecting ATP production in EA.hy926 cells measured as a time to cell lysis
479 in response to NaCN (1 mM) and IAA (20 µM). Data are presented as means ± SEM. The differences
480 were not statistically significant ($P < 0.05$).

481 **Figure 3**

482 **CORM-401 induces slight mitochondrial depolarization**. Mitochondrial membrane potential changes
483 in time were determined in EA.hy926 cells treated with 30 µM CORM-401 (A, n = 35 cells) or 30 µM
484 iCORM-401 (B, n = 73 cells) by Rhodamine-123 (10 µM) fluorescence in a dequenched mode. (C)
485 Mitochondrial membrane potential 10 min after incubation of cells with CORM-401 or iCORM-401 in
486 comparison to untreated control was determined by TMRM (25 nM) fluorescence in a quenched
487 mode (data are presented as means ± SEM , $P < 0.05$). D and E are representative TMRM images of
488 control and CORM-401 treated cells. (F) ROS generation under CORM-401 in comparison to iCORM-
489 401 treatment measured by live cells imaging of hydroethidine (2 µM) fluorescence. (G) 2-OH-E+
490 level in EA.hy926 cells: control or incubated for 30 min with 30 µM CORM-401, 30 µM iCORM-401 or
491 10 µM menadione (as a positive control). Data are presented as means ± SEM of three independent
492 experiments, three replicates in each experiment (**$P < 0.01$).

493 **Figure 4**

494 **CORM-401 decreases participation of glycolysis-derived ATP in maintenance of $\Delta\Psi_m$**. Oligomycin
495 null-point test was performed with using TMRM (25 nM). $\Delta\Psi_m$ was measured in control EA.hy926
496 cells (A) or cells pre-incubated for 20 min with 30 µM CORM-401 (B). Oligomycin (2 µg/ml) was used
497 to inhibit ATP synthase, FCCP (1 µM) was used to depolarize mitochondria. Data are presented as
498 means ± SEM.

499 **Figure 5**

500 **CORM-401 activates mitochondrial respiration in endothelial cells**. (A) NADH autofluorescence was
501 measured after treatment of EA.hy926 cells with 30 µM CORM-401 or 30 µM iCORM-401. FCCP (1
502 µM) was used as an uncoupler to maximize mitochondrial respiration, whereas NaCN (1 mM) as an
503 inhibitor of complex IV to inhibit mitochondrial respiration. Data present representative traces from
504 three independent experiments. (B) NADH redox index reflects of the ratio of NADH is in its reduced
505 form. Data represent means ± SEM of three independent experiments (***P* < 0.005); CORM-401, n =
506 98 cells; iCORM-401, n = 57 cells. (C) NADH pool was calculated as a difference in autofluorescence
507 between two states of ETC: maximally accelerated after addition of FCCP and completely inhibited
508 after addition of NaCN; it reflects a total amount of available mitochondrial NADH. (D)
509 Autofluorescence of NADH and FAD measured simultaneously in EA.hy926 cells treated with CORM-
510 401 (n = 8 cells). Data are presented as means ± SEM.

511 **Figure 6**

512 **CORM-401 increases mitochondrial calcium signal in EA.hy926 cells**. (A) Changes in X-rhod-1
513 fluorescence demonstrate an increase in calcium signal in mitochondria in live cells stimulated with
514 30 µM CORM-401. Each trace represents the mitochondrial calcium level in a single endothelial cell.

515

Figures

Figure 1

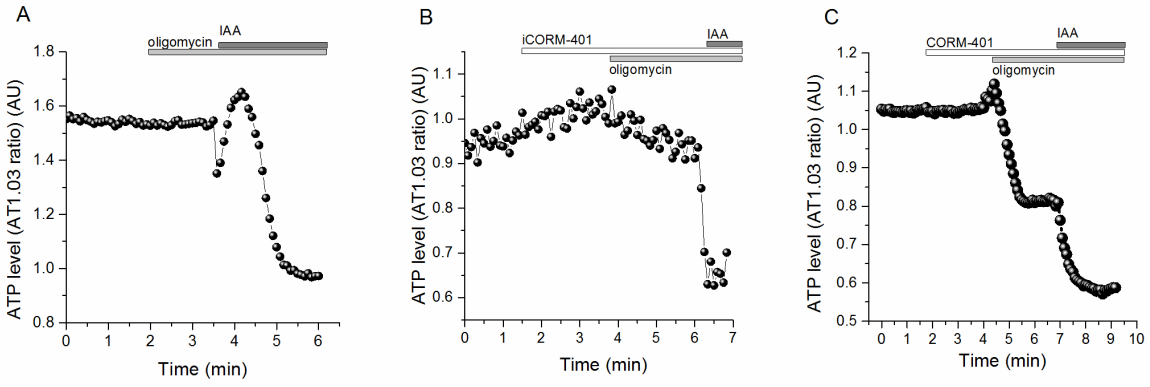

521

522 **Figure 2**

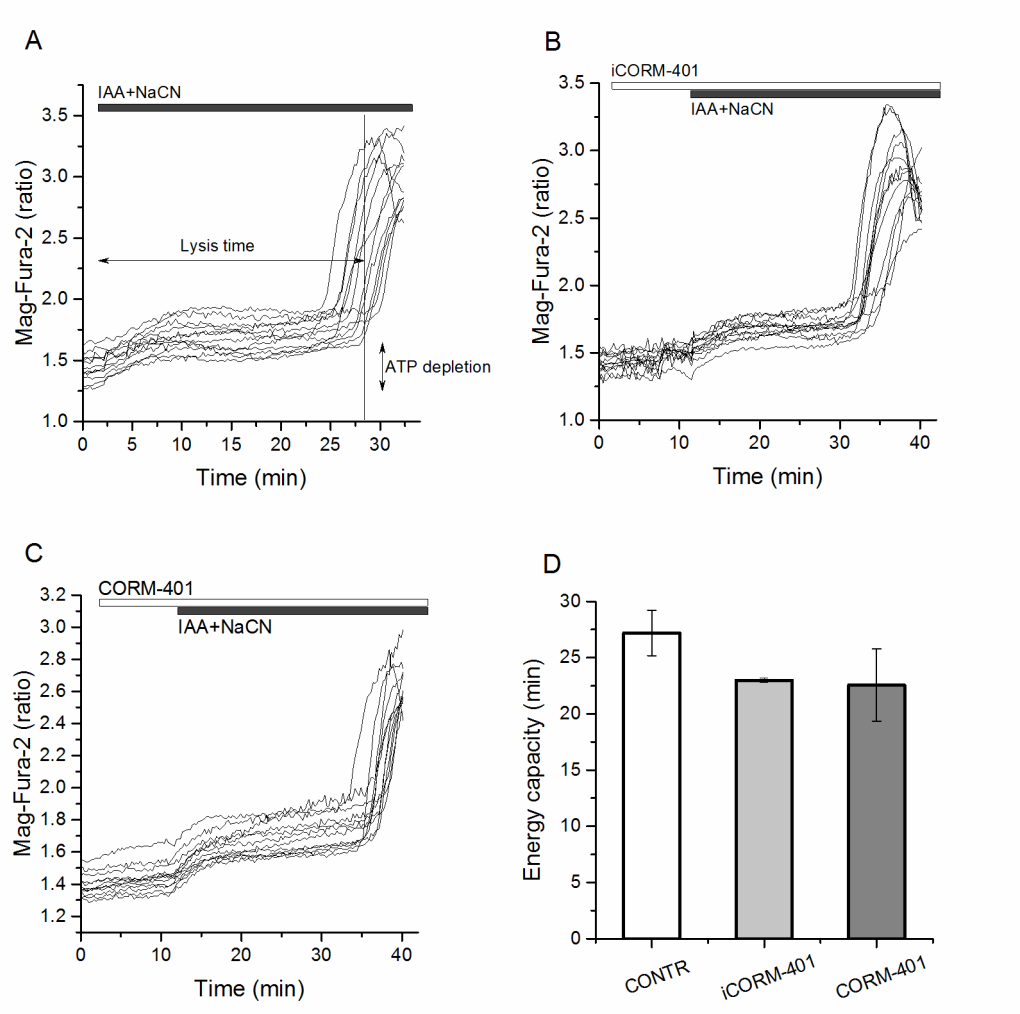

523

524

525

526 **Figure 3**

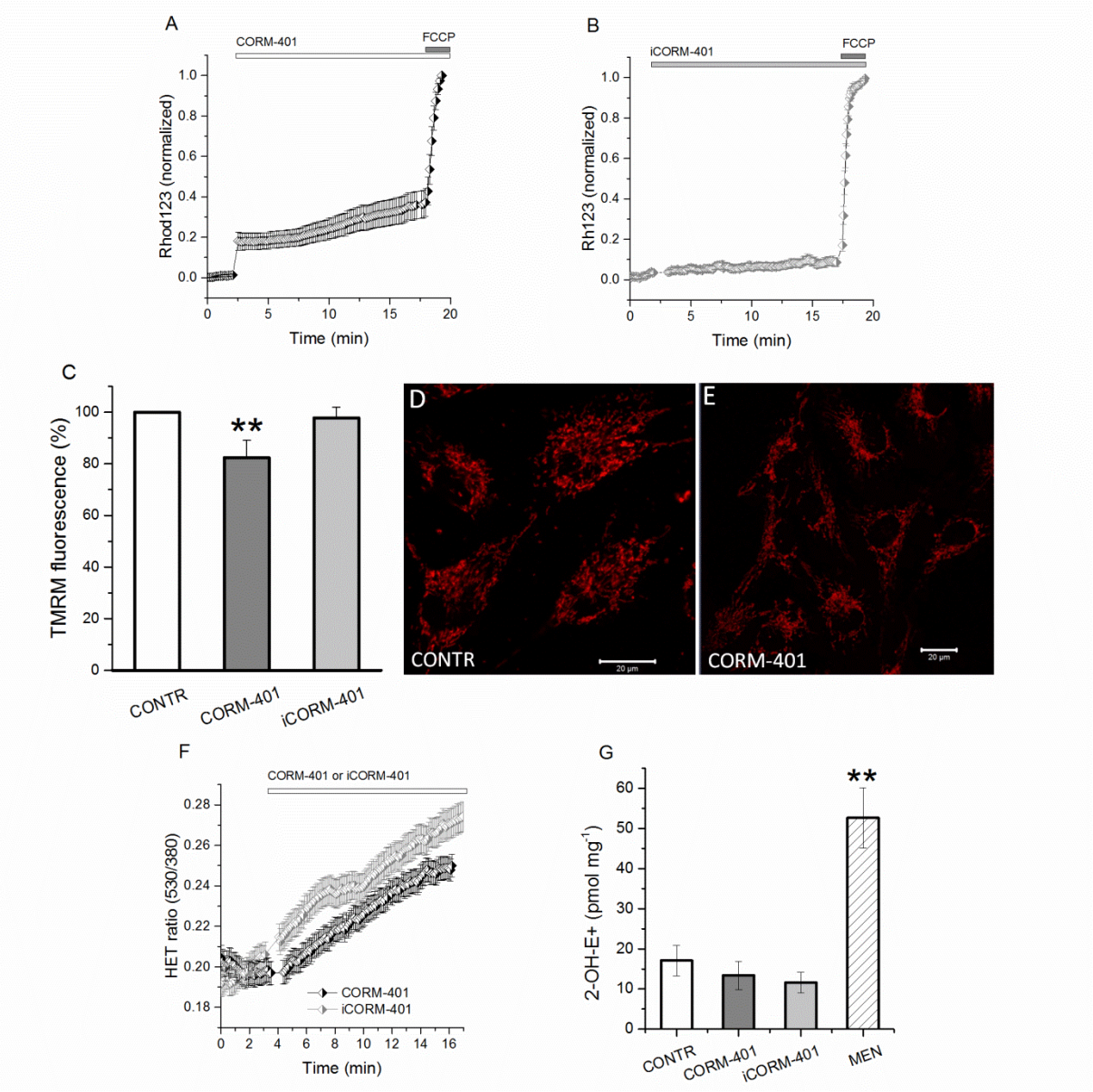

527

528

529

530 **Figure 4**

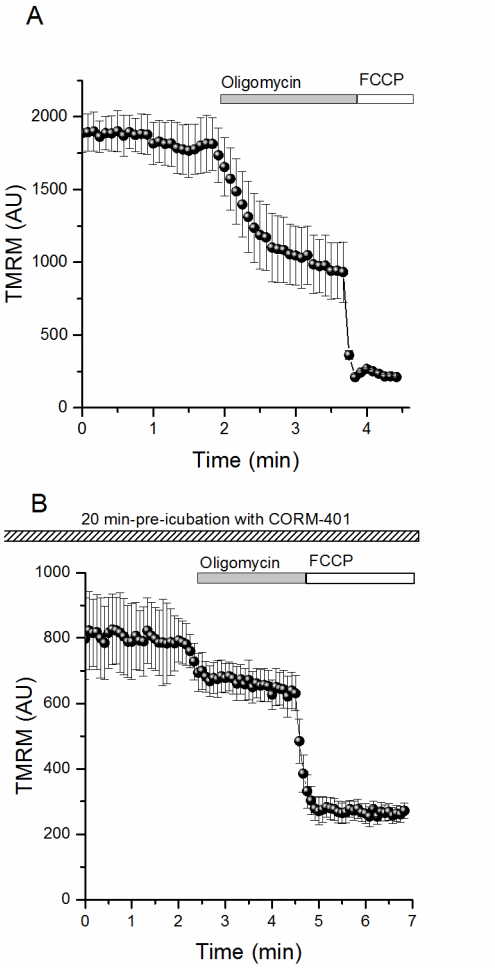

531

532

533

534 **Figure 5**

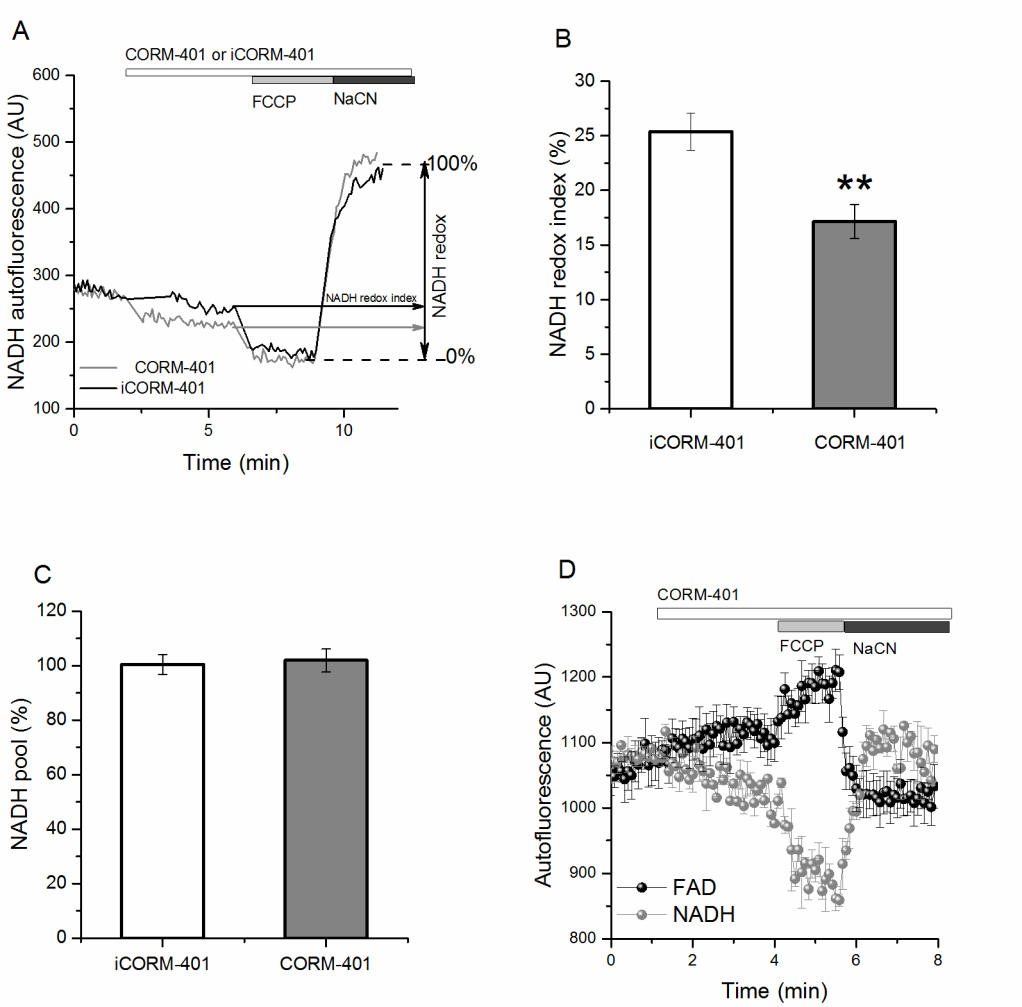

535

536

537

538 **Figure 6**

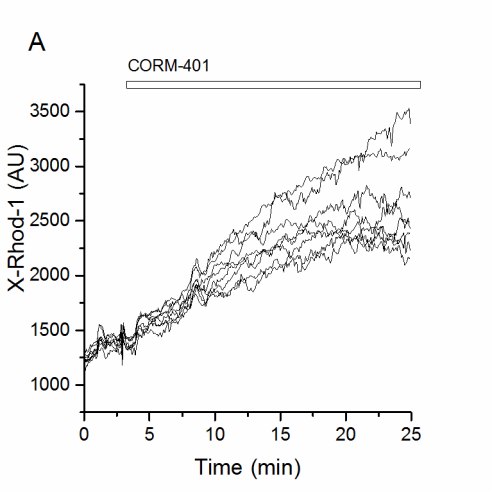

539